Zuse Institute Berlin

Takustr. 7
14195 Berlin
Germany

ALEXANDER LANGE, ROBERT SCHWIEGER,
JULIA PLÖNTZKE, STEFAN SCHÄFER, SUSANNA RÖBLITZ

Follicular competition: the selection of dominant follicles as a synergistic effect

ZIB Report 17-21 (May 2017)

Zuse Institute Berlin
Takustr. 7
14195 Berlin
Germany

Telephone: +49 30-84185-0
Telefax: +49 30-84185-125

E-mail: bibliothek@zib.de
URL: http://www.zib.de

ZIB-Report (Print) ISSN 1438-0064
ZIB-Report (Internet) ISSN 2192-7782

Follicular competition: the selection of dominant follicles as a synergistic effect

Alexander Lange,[1,2] Robert Schwieger,[3] Julia Plöntzke,[1]
Stefan Schäfer,[1] Susanna Röblitz [1,3]

[1] Computational Systems Biology, Zuse Institute Berlin
[2] Dept. of Appl. Biosci. and Process Engineering, Anhalt Univ. of Appl. Sciences
[3] Dept. of Mathematics and Computer Science, Freie Universität Berlin

E-mail: lange@zib.de

May 2017

Abstract

The estrous cycle of mono-ovulatory species such as cows or humans, is known to show two or more waves of follicular growth and decline between two successive ovulations. Within each wave, there is one dominant follicle escorted by subordinate follicles of varying number. Under the surge of the luteinizing hormone a growing dominant follicle ovulates. Rarely the number of ovulating follicles exceeds one. In the biological literature, the change of hormonal concentrations and individually varying numbers of follicular receptors are made responsible for the selection of exactly one dominant follicle, yet a clear cause has not been identified. In this paper, we suggest a synergistic explanation based on competition, formulated by a parsimoniously defined system of ordinary differential equations (ODEs) that quantifies the time evolution of multiple follicles and their competitive interaction during one wave. Not discriminating between follicles, growth and decline are given by fixed rates. Competition is introduced via a growth-suppressing term, equally supported by all follicles. We prove that the number of dominant follicles is determined exclusively by the ratio of follicular growth and competition. This number turns out to be independent of the number of subordinate follicles. The asymptotic behavior of the corresponding dynamical system is investigated rigorously, where we demonstrate that the ω-limit set only contains fixed points. When also including follicular decline, our ODEs perfectly resemble ultrasound data of bovine follicles. Implications for the involved but not explicitly modeled hormones are discussed.

Keywords differential equation models, follicular maturation, follicular waves, cows, humans

1 Introduction

Follicles, periodically growing and declining in the ovaries of female mammals, have a well-known function in the hormonal cycle. Besides providing the close environment for the oocytes to mature, they synthesize hormones that establish the feedback loop to the hypothalamus and pituitary in the estrous cycle, most importantly estradiol and inhibin [1]. Usually, follicles appear and grow in rather large numbers, even if eventually only one or a few—depending on the considered species—ovulate [2,3]. It has been argued that due to this fact follicles must interact and exchange information, they cannot grow following a random distributions alone [4]. The number of follicles growing and declining over one cycle is not fixed over consecutive cycles, this number can vary substantially [5], especially between individuals [6]. Possible explanations have been reviewed in [5], yet these facts remain puzzling. They form the biological content of this paper.

In the bio-mathematical literature that addresses follicular maturation [4,7–11], follicles have usually been modeled via the secreted amount of estradiol. This is the hormone that stimulates the synthesis of gonadotropins that keep the cycle running. Those early papers intended to formulate the non-linear kinetics of the follicles as a dynamical system, effectively covering the hormonal interaction of the whole

cycle. Modern systems-biological approaches focus on the hormonal dynamics (e.g., [12, 13]), where follicles are modeled as an abstract functional mass, sometimes representing certain stages of differentiation [14]. The histology of follicles has been modeled as well [15]. In [16], the time evolution of the hormone producing cells has been studied via reaction-diffusion processes. So far, however, follicles have not been described mathematically as seen in ultrasound scans of the ovaries, given by a set of diameters that change in size over time. This is what we intend to do here by defining and solving a system of ordinary differential equations.

There is evidence that, at least for the period of growth, follicular dimensions and amounts of synthesized hormones correlate [17]. That is, once, when knowing more about the time evolution of follicular diameters, such correlations could be utilized in order to couple follicular- and hormonal dynamics. For now, we are only interested in modeling a cohort of follicles and in predicting their individual diameters over time. Why do we choose such an approach? We suspect that the laws of growth and decline and the law of follicular interaction—being separated of each other—are both simple, simpler than the effective laws that have been suggested in the literature so far [4, 10].

For follicular growth and decline we will employ the simplest possible model that only involves spatial dimensions and is consistent with ultrasound data. Follicular interaction will be introduced as being proportional to a fraction of the follicular volume, intended to represent a hormone producing compartment. We will study how many dominant follicles develop under the proposed interaction, that is, follicles that are large and differentiated enough to be able to undergo ovulation. We determine the parameters that influence the selection of these follicles. We will investigate whether the number of dominant follicles is independent of the number of initially growing antral follicles. This will be done rigorously in a methods section at the end of the paper, once the models are formulated. Of course, we will present and discuss our mathematical results also verbally. But before, we provide some more biological background.

2 Background

In many mammals such as cows or humans (at which we look more closely here), females are born with a huge number of primordial follicles resting in their ovaries. This number decreases over time; in humans, from ca. 10^6 down to 5×10^5 at puberty [18]. Each of these follicles contains a premature oocyte that is surrounded by a few supporting cells. Continuously, starting at puberty, smaller sets of immature, primordial follicles develop further while undergoing a few stages of differentiation. In humans, this happens over a period of about one year. Only in their final stage, follicles are responsive to hormones, which are metabolized in granulosa- and theca cells surrounding the oocyte. By then a fluid-filled cavity adjacent to the oocyte has been formed, called antrum.

Under the influence of the follicle stimulating hormone (FSH), antral follicles are recruited to grow further. In humans, the number of recruited follicles is usually around 15, or below, depending on the age of the woman; their diameters are about 2 mm. Similar parameters apply to bovine follicles [19]. Both species are mono-ovulatory, that is, the number of dominant follicles rarely exceeds one, leading to only one offspring per pregnancy. Being able to control the number of dominant follicles is an important modeling goal in the context of reproductive medicine [20].

Over one cycle, several follicles are recruited, grow and decline. In woman, one observes up to three follicular waves with different dominant follicles [21,22]. In cows, the number of waves can be four or even five [23–25]. Only dominant follicles are assumed to ovulate [5], and only once per cycle,[1] when the level of the luteinizing hormone (LH) is sufficiently high. Ovulated follicles transform into a corpus luteum. From wave to wave, the number of antral follicles varies, yet, remarkably, the number of dominant follicles is almost always one. Of course, this only applies to mono-ovulatory species, such as cows or humans. For multi-ovulatory species, such as pigs [26] or hamsters [27], the number of dominant/ovulating follicles is higher, although it is narrowly distributed around a particular value specific to the considered species [28], which is far smaller than the number of initially growing antral follicles [7].

The first model that has reproduced the outlined behavior, at least approximately, was given by Lacker [4]; it is defined by a system of ODEs,

$$\dot{x}_i = x_i\big(1 - (\Sigma x - M_1 x_i)(\Sigma x - M_2 x_i)\big)\,, \quad i \le n\,, \tag{1}$$

[1] The rare exception is known as superfecundation.

where $x_i(t)$ represents the estradiol produced by follicle i at time t and $\Sigma x = \sum_{i=1}^{n} x_i$ the resulting total amount. The right hand side (r.h.s.) incorporates the dynamics of n equally interacting follicles by a polynomial of order three, capturing growth conditions imposed by the hormones, FSH and LH, in terms of two parameters, M_1 und M_2. These parameters are the same for all follicles.

Consecutive work has addressed some generalization [8, 9] and specialization [10, 11]. Soboleva et al. [10], e.g., claim they have specialized Lacker's model by utilizing a polynomial of order four on the r.h.s.,

$$\dot{x}_i = \frac{k\lambda^2}{E}(E - x_i)\, x_i \left(\lambda^2 - \Sigma x\,(\lambda - x_i)\right), \quad i \leq n\,, \tag{2}$$

defined by three positive parameters (E, k, λ), where E represents the maximum level of estradiol, k the scaling of time, and λ a production rate threshold. As long as follicles are small (i.e., total estradiol levels low, $\Sigma x < \lambda$), follicular growth—determined by the r.h.s.—is positive, although individual growth turns negative when some of the follicles become large. For large follicles ($x_i > \lambda$) growth is always positive. These features, which are encoded rather explicitly by the threshold λ, model the selection of dominant follicles in [10]. As in Lacker's model, the number of dominant follicles is variable, depending on the three parameters. That is, different species can be modeled, e.g., cows or sheep. For neither of the two models, however, the number of dominant follicles is given by an explicit formula. This does not surprise, as in both models this number depends on the initial conditions and, when mathematically precise, also on the total number of recruited antral follicles, n.

As indicated above, rising FSH levels prior to a follicular wave cause the recruitment [29] of late antral follicles and possibly their early growth [30]. However, as soon as follicles start to grow, FSH levels fall governed by the circular dynamics [31, 32]. In the bio-medical literature [32], falling FSH levels are made responsible for the selection of dominant follicles. Namely, when FSH is kept at high levels, artificially, follicles do not decline (FSH is anti-apoptotic [32], p. 51), and the selection of dominant follicles is suppressed by halted follicular growth. In [10], dominant follicles are selected when passing the threshold λ, and high exogenous FSH levels are modeled via a controlled reduction of Σx in the polynomial on the r.h.s.

It is not well understood how FSH can control follicular development. Maybe other hormones are involved as well and directly or indirectly suppress follicular growth. Follicles produce androgens, which are converted into estradiol, and thus establish a negative feedback in the estrous cycle. In the bio-medical literature [33], follicular interaction is also interpreted as competition, but truly competitive dynamics have not been utilized by models so far.

3 Models and results

In this paper, we model one follicular wave of the estrous cycle. Following an approach similar to Lacker [4] and Soboleva et al. [10], we assume that the follicles of that wave behave identically and are thus defined by the same set of parameters (a subset of $\eta, \gamma, \kappa, \nu, \rho, \xi \geq 0$). That is, we do not account for possible physiological differences. In contrast to that literature though, we study follicular diameters over time (denoted by $x_i(t)$, $i \leq n$), as being observable via ultrasound. We do not follow the amounts of estradiol the follicles produce, nor do we rely on other reproductive hormones involved in the estrous cycle such as FSH, LH, progesteron, or inhibin. Though we explain how administered FSH—implemented via the strength of competition—influences the growth of follicles.

Despite being identical in function, follicles usually differ in progression of their individual development (on the scale of hours). That is, when follicles start to grow during their final stage before ovulation, their diameters differ in size, at least slightly. Therefore, we propose that

$$\xi > x_1(0) > \cdots > x_n(0) > 0\,, \tag{3}$$

where ξ defines the *largest possible diameter* of a follicle and n the *total number of antral follicles*. We refer to those $x_i(0) \in (0, \xi)$, $i \leq n$, restricted by (3) as *generic* initial conditions (GICs).

Even if our model is applicable to many different mammals, we will compare our theoretical results to follicular data of cows [25] and adapt the numerical parameters accordingly.

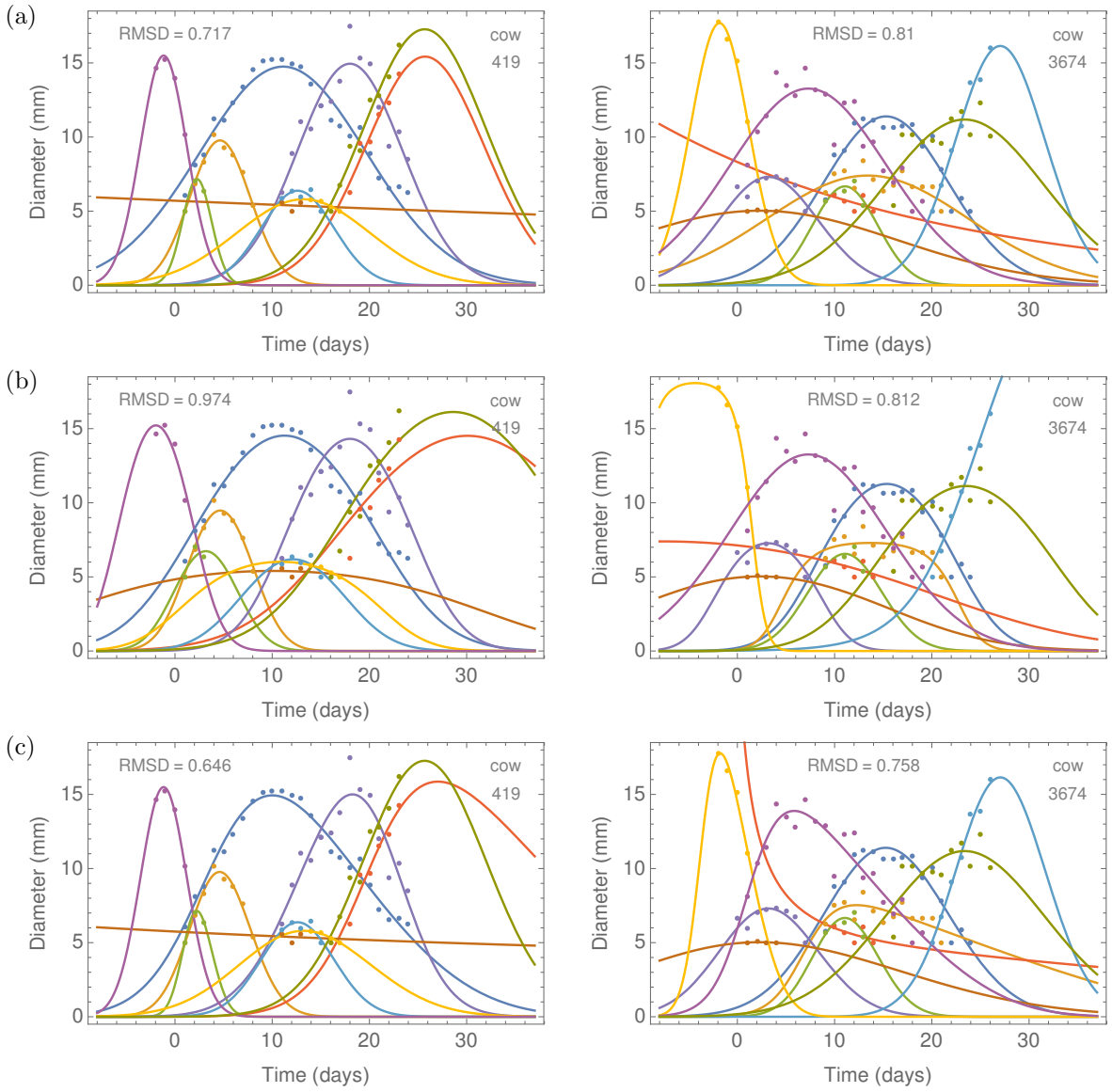

Figure 1: Ultrasound data of follicles approximated by bell-shaped trajectories over one estrous cycle. Follicular diameters of two arbitrarily chosen cows from [25] are fitted in (a), (b), (c) by the models (4), (5), (6), respectively. Parameters are numerically optimized for each follicle individually. The root-mean-squared deviations (RMSD) are given for each method with respect to all data of one cow. The best fit is achieved by modeling logistic growth and simple decline (6), which is followed by bell-shaped Gaussian growth and decline (4). Even for the loosing method, which models logistic growth and decline (5), the average deviation is less than 1 mm per measurement.

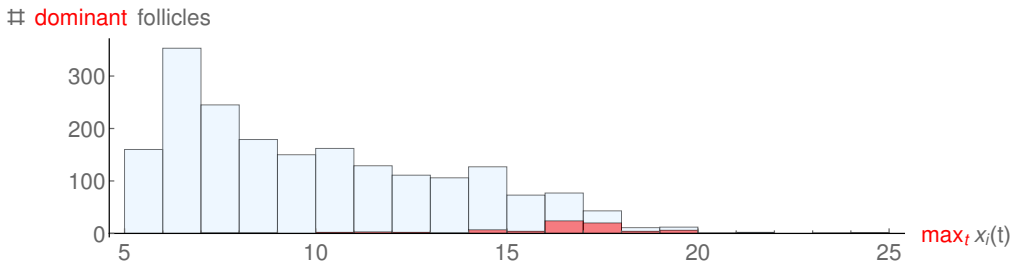

Figure 2: Distribution of (maximal) follicle diameters. The histogram shows the distribution of the follicle diameters (gray) and the maximal diameters of dominant follicles (red) of all 31 cows in [25]. The diameters of all 1943 follicles rarely exceed 18 mm, exactly 26 times. The maximal diameters of 45 of 77 dominant follicles lie within the range of 16–18 mm.

3.1 Follicular kinetics

During their final stage before ovulation antral follicles grow fast. Dominant follicles, for example, extend their diameter by about one order of magnitude within one week. Similarly fast they decline again.[2] The simplest model that captures such a behavior—for both dominant and subordinate follicles—is given by

$$\dot{x}_i = x_i\ (\gamma - \rho\, t)\ , \quad i \leq n\,, \tag{4a}$$

where $\gamma > 0$ and $\rho > 0$ define *rates of growth* and *decline*, respectively. The solutions, which fit bovine data fairly well (cf. Fig. 1), are given by bell-shaped trajectories,

$$x_i(t) = x_i(0)\, e^{-\frac{\rho}{2}\, t^2 + \gamma\, t}\,. \tag{4b}$$

The maximal diameter of follicles only varies within a small range (highlighted red in Fig. 2). Therefore, one might improve (4a) by including a term that yields logistic behavior,

$$\dot{x}_i = (\xi - x_i)\ x_i\ (\gamma - \rho\, t)\ , \quad i \leq n\,, \tag{5a}$$

where ξ defines an upper bound for the follicle diameter. The solution of these ODEs reads

$$x_i(t) = \frac{\xi}{1 + \left(\frac{\xi}{x_i(0)} - 1\right)\ e^{\frac{\rho}{2}\, t^2 - \gamma\, t}}\,. \tag{5b}$$

In fact, numerically, the resulting fit (cf. Figs. 1 and 3) does not approximate ultrasound data better than bell-shaped Gaussian curves (4b). But the fit via (5b) models the more typical set of trajectories (Fig. 3b): usually, follicles of a particular wave originate from a common trajectory before subordinate follicles branch off (below the trajectory of a dominant follicle) [25, 32, 34, 35]. All bell-shaped curves (Fig. 3a), in contrast, clearly start at different points.

When looking at the follicle data more closely (cf. Figs. 1c and 3c) one sees that, for large follicles, decline takes longer than growth. To account for that observation one could model logistic behavior only for follicle growth and not for decline,

$$\dot{x}_i = x_i\,((\xi - x_i)\gamma - \rho\, t)\ , \quad i \leq n\,. \tag{6a}$$

This would lead to an analytic solution as well,

$$x_i(t) = \frac{e^{-\frac{\rho}{2}\, t^2 + \gamma\, \xi\, t}}{\frac{1}{x_i(0)} + \frac{\sqrt{\pi}\gamma}{\sqrt{2\rho}} e^{\frac{\gamma^2 \xi^2}{2\rho}} \operatorname{erf}\left(\frac{-\gamma\xi}{\sqrt{2\rho}}, \frac{\rho t - \gamma\xi}{\sqrt{2\rho}}\right)}\,, \tag{6b}$$

[2] This also applies to ovulating follicles, which decline in size when releasing the oocyte, before transforming into a corpus luteum.

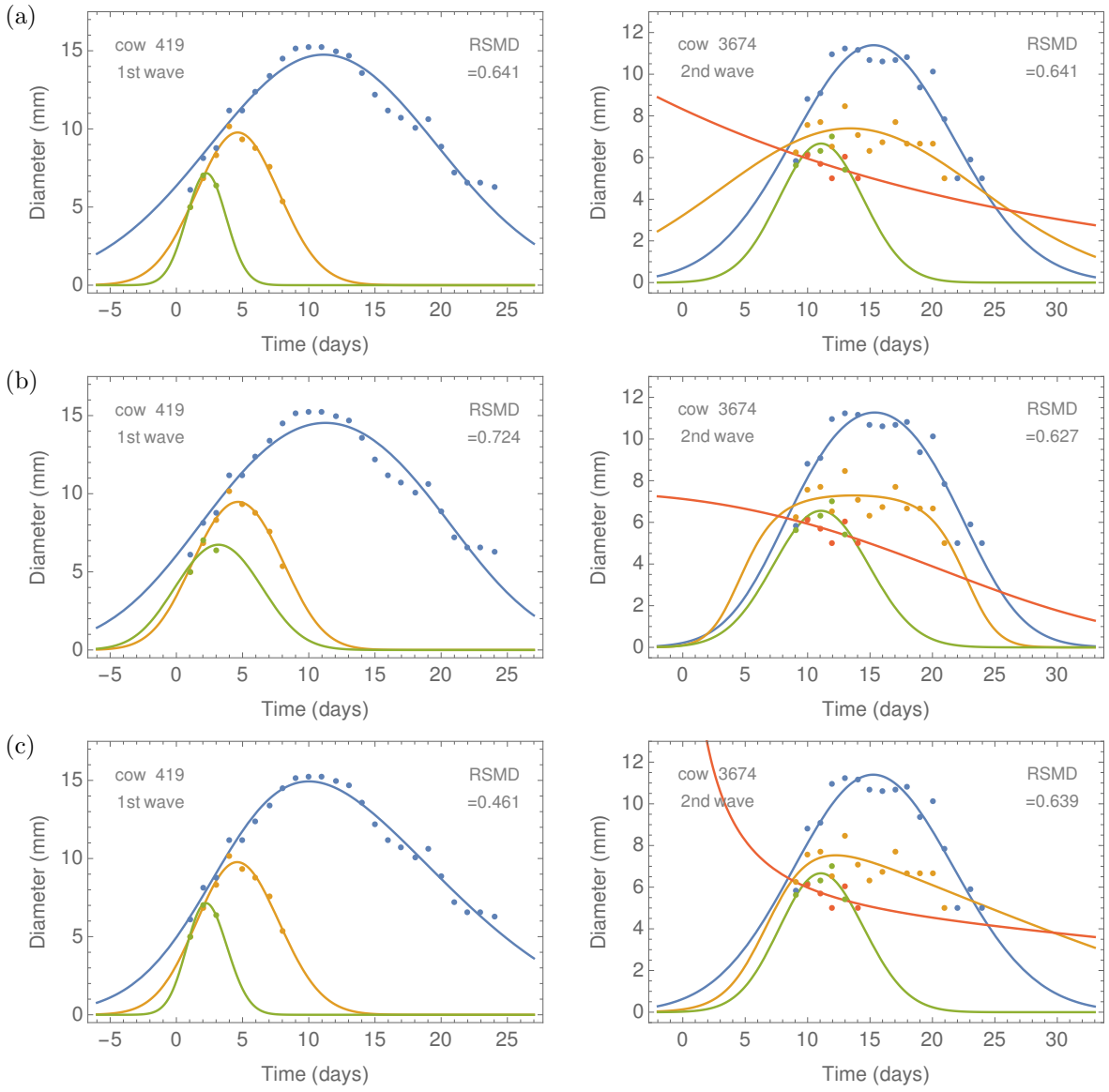

Figure 3: Bell-shaped versus logistic growth. This figure shows individual follicular waves (data and least square fit of the first and second wave) of the two cows in Figure 1; the enumeration of the panels is the same. The only difference is the evaluation of the fits. For individual waves (cow 3674, 2nd wave), logistic growth and decline (5) can outcompete the other two methods, (4) and (6). In fact, the follicular peak is usually softer than a Gaussian bell-shaped curve. Furthermore, all growing follicles usually evolve following the trajectory of the dominant follicle before subordinate follicles branch off. Trajectories with logistic behavior better account for these two qualities.

although the solution requires numerical integration and is thus impractical to use; it contains the error function $\mathrm{erf}(a,b) = \frac{2}{\sqrt{\pi}} \int_a^b e^{-t^2}\, dt$. The fit is the best among the three models.

Our results indicate that follicular growth likely follows logistic behavior; one may note that Soboleva et al. [10] have also incorporated a logistic term (2). But it is difficult to decide which of our two versions should be favored. The solutions of (6) yield the better fit (on average; cf. Fig. 3c), but the solutions of (5) represent a more realistic starting behavior (with trajectories being closer together; cf. Fig. 3b).

The fits in this subsection have been produced with a large set of follicle-dependent parameters. In order to describe multiple follicles with a small set of follicle-independent parameters one must include interaction between follicles.

3.2 Competitive growth

Interaction between follicles is considered in the models of Lacker [4] and Soboleva et al. [10]. Their dynamical equations incorporate the sum, $\Sigma x = \sum_{i\le n} x_i$, which represents the total amount of estradiol produced by the follicles. When studying follicular diameters (as we do here), it is more realistic to consider the sum of certain powers of the individual diameters, $\Sigma x^\nu = \sum_{i\le n} x_i^\nu$. This sum represents a multiple of the total follicular volume (of fractal *dimension* $\nu \le 3$), which can easily be related to the amount of hormones that are produced. We assume that these hormones (e.g., androgens or their derivatives such as estradiol) directly or indirectly suppress the growth of follicles, though we expect that individual follicles do not fully suppress their own growth.

Suppressed growth, implemented in (5a) by an additional negative growth rate,

$$-\kappa \left(\sum_{\substack{j=1 \\ j\neq i}}^{n} x_j^\nu + \eta x_i^\nu \right) = -\kappa \left(\Sigma x^\nu - \mu x_i^\nu \right), \tag{7}$$

is our model for follicular competition. The dynamical system of *competitive growth* reads

$$\dot{x}_i = (\xi - x_i)\, x_i \left(\gamma - \kappa \left(\Sigma x^\nu - \mu x_i^\nu \right) \right), \quad i \le n, \tag{8}$$

where κ defines the *strength of competition*, and the parameter $\mu = 1 - \eta$ incorporates the *proportion of self-harm* $\eta \in (0,1)$. Of course, we must consider at least two follicles, i.e., $n \ge 2$. There are no analytic solutions to this system of ODEs. Rigorously, one can only determine its asymptotic solutions for large time. We find that these solutions converge towards fixed points.[3] This can be proven as a mathematical statement.

Theorem. *Let* $0 < \eta = 1 - \mu < 1 \le \nu$ *and* $n \ge 2$. *Then any solution of the ODE-system* (8) *satisfying generic initial conditions* (3) *converges to the stable fixed point*

$$\big(\underbrace{\xi, \dots, \xi}_{d}, \xi^-, \underbrace{0, \dots, 0}_{n-1-d} \big)^{\mathsf{T}} \in \mathbb{R}^n \quad as \quad t \to \infty, \tag{9}$$

where $\xi^- = \min\big\{1, \max\big\{\frac{\delta - d}{\eta}, 0\big\}\big\}^{1/\nu} \xi$ *and*

$$d = [\delta + \mu] \quad with \quad \delta = \frac{\gamma}{\kappa}\, \xi^{-\nu}. \tag{10}$$

The bracket $[\cdot]$ *denotes the integer part.*

Proof. This is the content of the methods section. For illustration, see Figure 4a. □

The integer $d \ge 0$ represents the number of *dominant follicles* (a lower bound, to be precise). This number is controlled by the parameter δ, which incorporates the ratio γ/κ of growth and competition (taken with respect to the largest possible hormone producing volume, i.e., $\propto \xi^\nu$). Importantly, these parameters are independent of the total number of antral follicles that define the wave. Among these n follicles, there might be one (and only one) that is neither growing towards ξ nor vanishing at infinity. Its

[3] i.e., there are no limit cycles, etc.

diameter is given by $\xi^- \in [0, \xi)$; see the yellow trajectory in Figure 4a (l.h.s.). This happens when $\delta > d$. Whether this follicle is dominant or subordinate remains undecided and may depend on the particular case (cf. Sect. 3.5 below).

Before the trajectories of the follicular diameters converge towards a stable fixed point (as stated in the theorem) they are bent by an unstable fixed point,

$$x_i^* = \frac{\gamma}{\kappa}\,(n+\mu)^{-1/\nu} =: \xi^+\,, \quad i \le n\,. \tag{11}$$

For illustration, see Figure 4; initially the trajectories gather around the dotted line at ξ^+. For proof, see the end of the methods section.

3.3 Comparison of models

After formulating our competitive growth model (8) we made a surprising observation. The model (2) by Soboleva et al. [10] can be written in terms of the parameters used in (8),

$$\dot{x}_i = (\xi - x_i)\,x_i\,\big(\gamma - \overbrace{\underbrace{\Sigma x^\nu}_{\text{interchanged positions}}\big(\underbrace{\kappa}_{} - \mu\,x_i^\nu\big)}^{\text{interaction term}}\big)\,, \quad i \le n\,, \tag{12}$$

where $\xi = E$, $\gamma = k\lambda^4/\xi$, $\kappa = \gamma/\lambda$, $\mu = \kappa/\lambda$, and $\nu = 1$. Despite the differing conceptual approaches, the two models, (12) and (8), look very similar. The only difference are the positions of the parameters Σx and κ, where the former represents competition and the latter its strength (here) or a growth threshold (in [10]). The positions of the parameters are simply interchanged, which, however, identifies the models as markedly different. In Soboleva et al (12), the interaction term does not have a fixed sign: if the sign is positive, it supports growth, if the sign is negative (i.e., $x_i < \kappa/\mu$), it suppresses growth (and determines subordinate follicles). In our model (8), the sign is always negative. That is, Soboleva et al model the selection of dominant follicles via the threshold κ/μ. We model the selection via dynamic competition, adjustable in strength κ and self-harm $\eta = 1 - \mu$.

3.4 Follicle stimulating hormone

The relationship between follicular growth and FSH involves another important similarity and difference of the two models. In the model of Soboleva et al (2), FSH—being included to simulate fertility treatment—is implemented by redefintion of the follicle sum, $\Sigma x^\nu \to \Sigma x^\nu - f_{\text{FSH}}^{(2)}$, via a term $f_{\text{FSH}}^{(2)}$ that monotonously depends on the amount of FSH exogenously provided to the system [10]. In our model (8), we would—in complete analogy—redefine the strength of competition, $\kappa \to \kappa - f_{\text{FSH}}^{(8)}$, via a similar term $f_{\text{FSH}}^{(8)}$ that monotonously depends on the exogenous FSH.

Supplementation of FSH is an essential part of fertility treatment protocols [36], leading to an increased number of dominant follicles. The mechanism behind is not fully understood. In [32], it is even argued that FSH suppresses the selection of dominant follicles. Our formula (10) and its FSH-supplemented version,

$$d_{\text{FSH}} = \left[\xi^{-\nu}\frac{\gamma}{\kappa - f_{\text{FSH}}^{(8)}} + \mu\right]\,, \tag{13}$$

can explain how treatment may work: $d_{\text{FSH}} > d$ whenever $f_{\text{FSH}} > 0$. That is, exogeneous FSH increases the number of dominant follicles.

3.5 Follicular kinetics with competition

By including the competition term (7) into the follicular kinetics equations, (5a) and (6a), which both involve logistic growth (as argued in Sect. 3.2) but either logistic or simple decline, one obtains two alternative models for the evolution of follicle diameters over one follicular wave,

$$\dot{x}_i = (\xi - x_i)\,x_i\,(\gamma - \kappa\,(\Sigma x^\nu - \mu x_i^\nu) - \rho\,t)\,, \qquad i \le n\,, \tag{14}$$

$$\dot{x}_i = (\xi - x_i)\,x_i\,(\gamma - \kappa\,(\Sigma x^\nu - \mu x_i^\nu)) - \rho\,t\,x_i\,, \qquad i \le n\,. \tag{15}$$

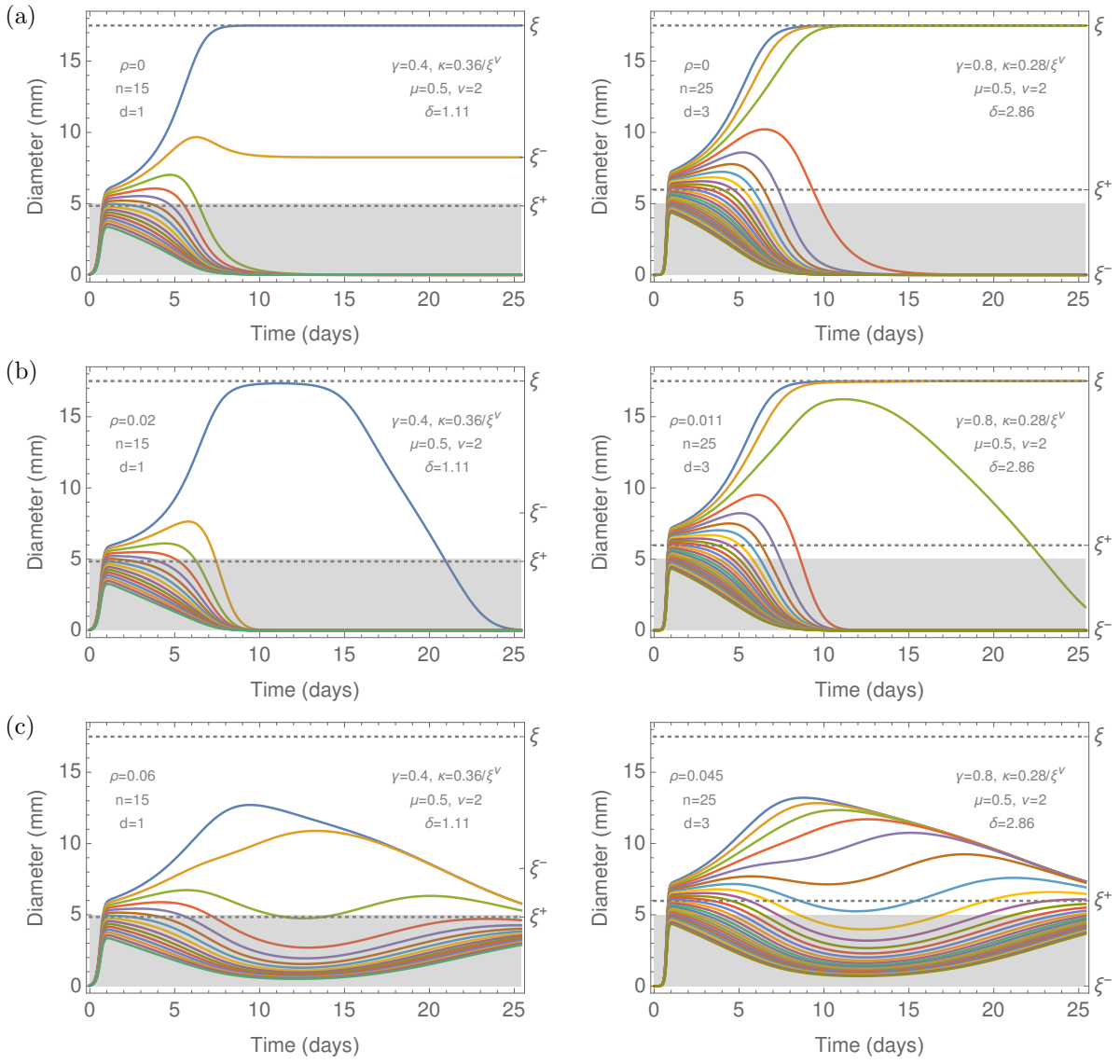

Figure 4: Model trajectories. Numerical solutions to the initial value problem with GICs are illustrated for the model of competitive growth (8) (Panel a), for the model of logistic growth and logistic decline (14) (Panel b), and for the model of logistic growth and simple decline (15) (Panel c). The plots show typical trajectories of follicle diameters for two different numbers of dominant and antral follicles (1 and 15 on the l.h.s., 3 and 25 on the r.h.s.), resulting from two different parameter sets. The gray area shows the region that is invisible by the ultrasound data we use [25].

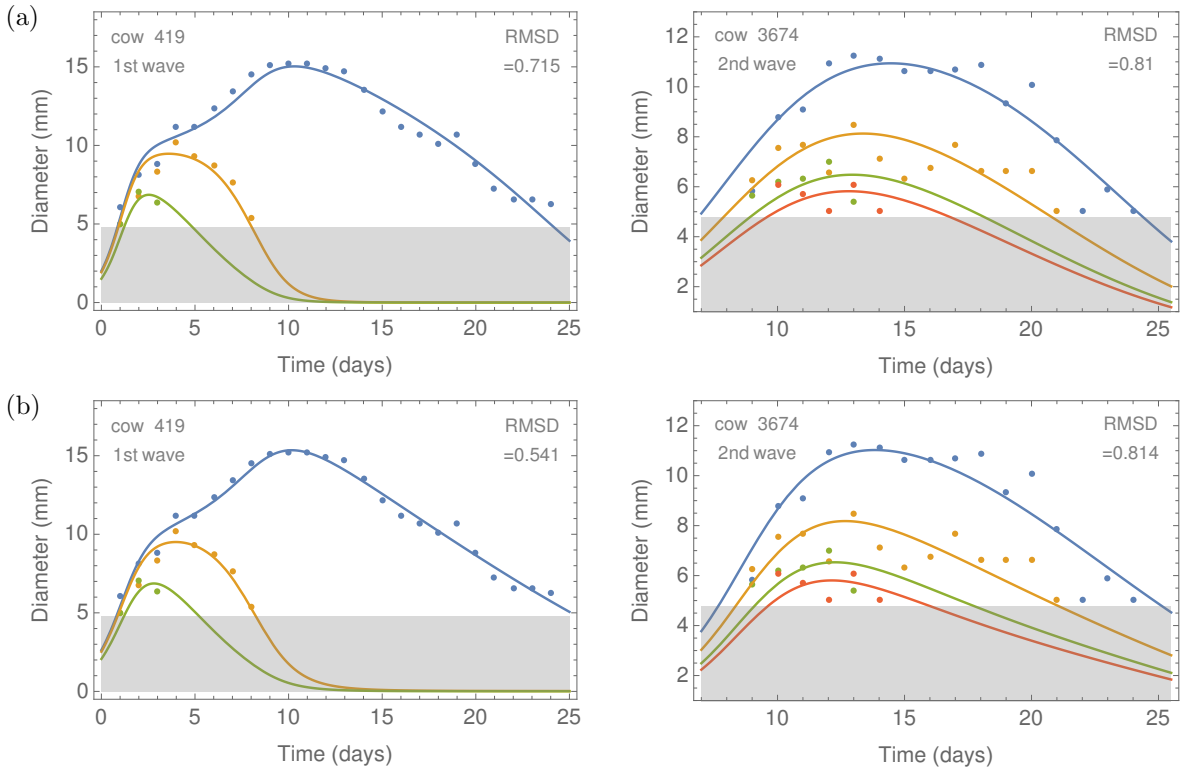

Figure 5: Follicular kinetics with competition versus data. Follicle diameters of two cows (the same as in Figs. 3b and 3c) during the first (l.h.s.) and second follicular wave (r.h.s.) are approximated by the two competitive growth models: logistic decline (14) in Panel (a) and simple decline (15) in Panel (b). The initial time for the second wave has been set to day 8. Six parameters ($\eta, \gamma, \kappa, \nu, \rho, \xi$; cf. Fig. 6) as well as three (l.h.s.) and four initial values (r.h.s.) have been optimized, numerically, to achieve the best possible least square fit; RMSD indicates the root-mean-squared deviation.

Both systems of ODEs can only be solved numerically; see Figure 4b and 4c. After looking at the resulting trajectories and comparison with some veterinary literature [25,32,34,35], where without supplementation of hormones declining diameters have not been reported to increase again [37] (or to converge towards a common trajectory as seen in Figure 4c), one might think of excluding simple decline (15) as modeling candidate of follicular dynamics.

Reality, however, is not that simple [38]. Both candidates lead to beautiful fitting results; see Figure 5. In fact, simple decline (15) even outperforms logistic decline (14) in our first-wave example (l.h.s. panels); in the second-wave example (r.h.s. panels) both models perform equally well. Though we think that for multiple dominant follicles one will favor logistic decline. This conjecture is based on the trajectories obtained in Figure 4, where, as discussed in Sect. 3.1, Panel (b) offers the most realistic shapes.

By inspecting the parameters (Fig. 6) that establish the fit of the follicle data (Fig. 5) we find an example where our follicle formula (10) only provides a lower bound (cf. end of Sect. 3.2). For logistic decline (15), the first follicular wave (l.h.s. panels of Figs. 5 and 6) is approximated best by a set of parameters that leads to $\delta > d = 0$. But, despite $d = 0$, there does exist one real dominant follicle of size smaller than $\xi^- > 0$. However, the best fit for simple decline (14) leads to a more predictive parameter set, where $\delta \leq d$ and $d = 1$ truly represents the number of dominant follicles.

4 Discussion and outlook

We have formulated and analyzed systems of ODEs that model the growth of follicles over a period of one follicular wave, covering follicular interaction and two versions of decline. In doing so, we have demonstrated that dominant follicles are selected from a cohort of growing antral follicles in a systematic and reproducible fashion when follicular interaction is based on competition. Our modeling framework allows for predicting the number of dominant follicles via a closed formula; see (10) and (13). The number only depends on the ratio between follicular growth and competition. In particular, it does not dependent on the number of recruited antral follicles. Numerically, we have adjusted our modeling parameters to cows, although other mammals such as humans, sheep, pigs, or hamsters, which in that order develop larger numbers of ovulating follicles, could be modeled as well (cf. Fig. 4). The trajectories of the follicular diameters fit ultrasound data amazingly well (Fig. 5).

Based on our modeling assumptions we were able to explain the selection of dominant follicles as a synergistic phenomenon, relying on competitive dynamics that penalizes individual follicles by suppression of growth. This suggests that selection may not rely on a particular threshold mechanism as proposed in Soboleva et al. [10] and may not be triggered, at least not directly, through an information processing network of chemicals as argued in the more experimental literature [29, 31]. The microbiological details (i.e., the way competition is mediated) may not be important for the selection itself. The strongest indicator supporting such an approach is the number of subordinate follicles that hugely varies between follicular waves. These subordinate follicles provide the reproductive system with a variable number of receptors, produce different amounts of hormones, etc. But, despite the involved variation, the selection process always leads to a well-defined number of dominant follicles, at least within a small range [28].

In nature, competition is likely mediated via androgens and estradiol, where the former are produced from steroid precursors in the theca cells, and the latter are converted from androgens in the granulosa cells of the follicles [39]. The corresponding dynamics could be as follows,

$$\dot{a}_i = \alpha \left(\frac{dx_i^\nu}{dt} \right)_+ - \beta\, a_i\,, \quad i \leq n\,, \tag{16a}$$

$$\dot{E} = \beta A - \omega E\,, \tag{16b}$$

where the rate of androgens $a_i(t)$ synthesized by follicle i at time t depends on the change of the productive follicular volume $x_i^\nu(t)$, and the amount of estradiol $E(t)$ synthesized at time t depends on the total amount of androgens $A = \sum_{i \leq n} a_i$ present at time t; the parameters $\alpha, \omega > 0$ define growth and decay rates of androgens and estradiol, respectively, and $\beta > 0$ defines the conversion rate. The index '+' represents the positive part, $(\,\cdot\,)_+ = (\,\cdot + |\cdot|)/2$. As long as the production of androgens and the conversion to estradiol balances, and provided decay rates are smaller than conversion (i.e., $\dot{a}_i \approx 0$, $\omega/\beta \approx 0$), one obtains a linear relationship between the follicular volumes and estradiol, $E = \alpha\, \Sigma x^\nu + const$, consistent with the models of Lacker [4] and Soboleva et al. [10].

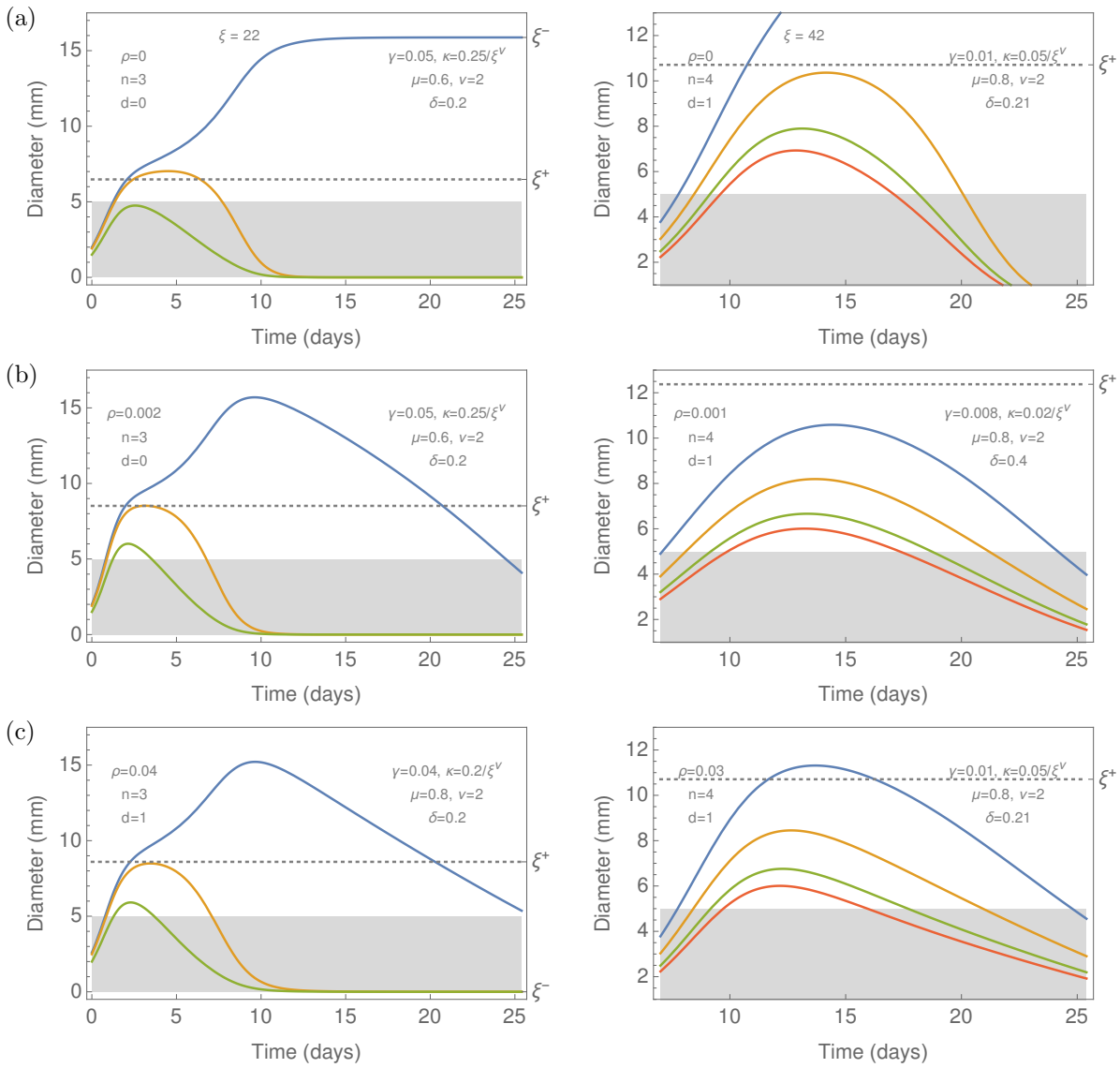

Figure 6: Follicular kinetics with competition. Panels (b) and (c) mirror the fitting trajectories of Figure 5b and 5c while indicating the involved parameter values. Panel (a) shows trajectories of the corresponding competitive growth model. For the visibility of the entire fixed point, ξ has been reduced from ca. 28 mm in (b) to 22 mm; the blue trajectory—representing a dominant follicle—converges towards ξ^-, which is below ξ but clearly above zero.

The previous statement is consistent with other claims in the literature, where the rise of estradiol [7] or the decline of FSH [16] is made responsible for the selection of dominant follicles. Consistency can be checked by comparison with the hormonal dynamics of the estrous cycle [1, 22, 40]. However, the follicle model we have developed does not require knowledge about the underlying hormones or the hormonal network and is thus available as a clean starting point for larger systems-biological models that couple diameters of individual follicles and reproductive hormones.

5 Methods

In this section, we prove our theorem while looking more closely at trajectories of the follicular diameters and their limiting behavior. For the mathematical treatment, we transform coordinates, $x_i \to \xi\, x_i$, and time, $t \to t/\kappa$. This leads to a system of ODEs and GICs, which are equivalent to (8) and (3), but contain two parameters less:

$$\dot{x}_i = g_i(x)\,, \qquad i \le n\,, \tag{17a}$$

where $n \ge 2$ and $g_i(x) = (1 - x_i)\, x_i\big(\delta - \Sigma_i(x)\big)$ with $\Sigma_i(x) = \sum_{j=1}^{n} x_j^\nu - (1-\eta)\, x_i^\nu$, and

$$1 > x_1(0) > \cdots > x_n(0) > 0\,. \tag{17b}$$

Furthermore, we assume that $0 < \eta < 1 \le \nu$.

5.1 Trajectories

The trajectories do not cross, nor touch in finite time. Furthermore, they are bounded. In mathematical terms this reads as follows.

Proposition 1. *The solution of the ODE-system with GICs (17) is order preserving and bounded within* $[0, 1]$ *(i.e.,* $1 > x_1(t) > \cdots > x_n(t) > 0$*,* $\forall t > 0$*).*

Proof. By contradiction: if two trajectories, $x_i(t)$ and $x_j(t)$ $(i \ne j)$, were touching at some time $t_0 > 0$ then, by symmetry of the ODE-system, $x_i(t) = x_j(t)$, $\forall t \ge t_0$. The backward time equation of (17a), $\frac{d}{dt}x(-t) = -g(x(-t))$, is also symmetric. Employing $x_i(t_0) = x_j(t_0)$ as initial condition, this would imply that $x_i(0) = x_j(0)$. Boundedness (i.e., $0 < x_i(t) < 1$, $\forall i \le n$) follows from Lipschitz continuity of $g_i(x_i)$, because $g_i(x_i) \to 0$ as $x_i \to 0$ or $x_i \to 1$. □

The solution either converges to zero ($x(t) \to 0$ as $t \to \infty$) or the trajectory enters the set $S = \{x \in [0,1]^n \,|\, g_1(x) \ge 0 \wedge x_1 > \cdots > x_n\}$ at some finite time $t_0 \ge 0$. The latter case only happens if $\delta > 0$, as shown further below. Importantly, for the statement we aim to prove, the trajectories do not leave the set S again (i.e., $x(t) \in S$, $\forall t \ge t_0$). That is, from a certain time on, the first component $x_1(t)$ will only increase. In mathematical terms this reads as follows.

Corollary 1. *The set* S *is an invariant set of the ODE-system (17a).*

Proof. Let $x \in S$. That is, the vector components of x are ordered and $g_1(x) \ge 0$. Then,

$$\delta \ge \sum_{j=2}^{n} x_j^\nu + \eta\, x_1^\nu \equiv \Sigma_1(x)\,. \tag{18}$$

Because of the proposition, one does not need to keep track of the order, one only needs to show that $g_1(x') \ge 0$, where $x' = x + h\, g(x)$ for a sufficiently small $h > 0$ [41]. That is, one must show that

$$\delta \ge \sum_{j=2}^{n} \big(x_j + h\, g_j(x)\big)^\nu + \eta \,\big(x_1 + h\, g_1(x)\big)^\nu =: \Sigma_1'(x)\,. \tag{19}$$

Two cases are possible. Case $g_1(x) > 0$. Condition (19) holds true, due to continuity of $\Sigma_1'(x)$ with respect to h. Case $g_1(x) = 0$. Here $\delta = \Sigma_1(x)$ and $\delta < \Sigma_j(x)$, $\forall j \ge 2$, as $x_1 > \cdots > x_n$ implies $\Sigma_1(x) < \cdots < \Sigma_n(x)$. That is, $g_j(x) < 0$, $\forall j \ge 2$, for any $h > 0$. Therefore, $\delta > \Sigma_1(x')$, i.e., $g_1(x') > 0$. □

Together with boundedness (Proposition 1), one immediately concludes that the first component of $x(t)$ converges to a number in $[0,1]$ as $t \to \infty$. That is, one obtains the following inclusion for the ω-limit set,

$$\lim_{\omega} \gamma_{x(0)} \subseteq \left\{ x \in [0,1]^n \middle| x_1 = x_1^* \right\} =: (x_1^*, *)\,. \tag{20}$$

By recursion this statement extends to all components, $x_i(t)$, and determines the ω-limit set to only consist of fixed points.

Lemma 1. *$x(t) \to x^* \in [0,1]^n$ as $t \to \infty$.*

Proof. Convergence of the solution of the n-dimensional system can be concluded, recursively, from the convergence of the first component,

$$x_1(t) \to x_1^* \in \begin{cases} \{0\} & \delta \leq 0 \\ (0,1] & \delta > 0 \end{cases}, \tag{21}$$

by successive elimination of this first component. Note that only the lower case in (21) is nontrivial. For $\delta > 0$, the first component $x_1(t)$ cannot converge to zero. If it did, one would be able to identify some $t_1 < \infty$ for which $\Sigma_1(x(t_1)) < \delta$, i.e., $g_1(x(t_1)) > 0$. By Corollary 1, $x_1(t)$ would then be increasing for all $t \geq t_1$, which would prove $x_1^* > 0$ and thus lead to a contradiction. Convergence in $(0,1]$ then follows from monotony on $[t_1, \infty)$ (Corollary 1) and boundedness (Proposition 1). Iterated formation of ω-limit sets applied to both sides of (20),

$$\lim_{\omega} \gamma_{x(0)} = \bigcup_{x \in \lim_\omega \gamma_{x(0)}} \lim_{\omega} \gamma_x \subseteq \bigcup_{x \in (x_1^*, *)} \lim_{\omega} \gamma_x\,, \tag{22}$$

and substitution of the growth parameter, $\delta^* = \delta - (x_1^*)^\nu$, enables us to study a system of only $n-1$ components,

$$\dot{x}_i = (1 - x_i)\, x_i \left(\delta^* - \left(\sum_{j=2}^{n} x_j^\nu - (1-\eta) x_i^\nu \right) \right), \quad i \in \{2, \ldots, n\}\,, \tag{23}$$

on the set $(x_1^*, *)$, alternatively to the n-component system (17a) defined on $[0,1]^n$. Since (23) has the same form as (17a), we can repeat the procedure and further reduce the number of components of the ODE-system until either $\delta^* \leq 0$ or no component $i \leq n$ is remaining. □

The asymptotic solution x^* must be one of the system's stable fixed points.

5.2 Fixed points

Fixed points $x^* = (x_i^*)_{i \leq n}$ of the system (17a) are defined by the requirement that its n right hand sides vanish: $g(x_i^*) = 0$, $\forall i \leq n$. That is, at least one of the three factors forming $g(x_i^*)$ must be zero. When applying the bounded monotonic behavior of the n trajectories (Proposition 1), the set of fixed points X^* is described as follows.

Lemma 2. *Assume that generic initial conditions (17b) apply. Then each fixed point of the ODE-system (17a) is given by*

$$x_i^* = 1 \qquad \forall i \in \{1, \ldots, d\} \tag{24a}$$

$$x_i^* = \left(\frac{\delta - d}{\eta + e - 1} \right)^{1/\nu} \in (0,1) \qquad \forall i \in \{d+1, \ldots, d+e\} \tag{24b}$$

$$x_i^* = 0 \qquad \forall i \in \{d+e+1, \ldots, n\}\,, \tag{24c}$$

for some natural numbers $d, e \geq 0$ satisfying either $d < \delta$ and $\delta + 1 - \eta < d + e \leq n$ or $d \geq \delta$ and $e = 0$. (Note that $[a,b] = \emptyset$ if $a > b$.)

Proof. The fixed points defined by (24b) and $e \geq 1$ are the only non-trivial ones. They are derived from the identity

$$0 = \delta - \sum_{\substack{j=1 \\ j \neq i}}^{n} x_j^{*\nu} - \eta\, x_i^{*\nu}, \qquad \forall i \in \{d+1, \ldots, d+e\}\,, \tag{25}$$

which—besides $(1 - x_i)$ and x_i—represents the third vanishing factor of $g(x_i)$. Written with the help of a matrix H, the identity reads

$$(\delta - d) \begin{pmatrix} 1 \\ \vdots \\ 1 \end{pmatrix} = H \begin{pmatrix} x_{d+1}^{*\,\nu} \\ \vdots \\ x_{d+e}^{*\,\nu} \end{pmatrix}, \tag{26}$$

where $H_{ik} = 1 + \eta\, \delta_{ik}$. As $\operatorname{rank} H = e$, there exists a unique solution for the vector $\left(x_{d+i}^*\right)_{i \leq e}$. Due to symmetry with respect to the index i, the entries of this vector are all the same: $x_{d+i}^* = x_{d+e}^* > 0$, $\forall i \leq e$. Summation over i yields

$$\begin{aligned} (\delta - d)\, e &= (\eta + e - 1) \sum_{i=1}^{e} x_{d+i}^{*\,\nu} \\ x_{d+i}^* &= \left(\frac{\delta - d}{\eta + e - 1} \right)^{1/\nu}, \qquad \forall i \in \{1, \ldots, e\}\,. \end{aligned}$$

This representation implies that $1 > x_{d+i}^* > 0$ is equivalent to $1 > \frac{\delta - d}{\eta + e - 1}$ (i.e., $\delta + 1 - \eta < d + e$) and $\delta - d > 0$. Recall that $e \geq 1$, which, because of the positivity of x_{d+e}^*, is leading to $\delta - d > 0$. That is, if $d \geq \delta$ then $e = 0$. □

Corollary 2. *Let $e = 1$. Then $d = [\delta]$ (where the square brackets denote the integer part, i.e., $\delta - 1 < d \leq \delta$ and $d \in \mathbb{N}$).*

Proof. It remains to show that $\delta - d < 1$. The following sequence of inequalities proves the claimed relation, $\delta - d = (\eta + e - 1)\, x_{d+e}^{*\,\nu} < \eta + e - 1 = \eta < 1$. □

We are interested in stable fixed points.

Proposition 2. *Let the limit set consist of the fixed points given by Lemma 2, and let x^* be any of those fixed points. Then x^* is stable if and only if one of the following disjoined conditions applies,*

(i) $\delta < d < \delta + 1 - \eta$,

(ii) either $\delta = d$ *or* $d = \delta + 1 - \eta$,

(iii) $\delta - \eta < d < \delta$ *and* $\eta < 1/\nu$.

For $\eta \geq 1/\nu$, either (i) or (ii) applies. For (i) and (ii), $e = 0$, and for (iii), $e = 1$.

Proof. Fixed points are characterized by the eigenvalues of the Jacobian J. That is, a fixed point is stable if the real part of the eigenvalues of J are all negative whereas a fixed point is unstable if at least one of the real parts of the eigenvalues of J is positive.

For our model (3), the entries of the Jacobian are given by

$$J_{ik}(x) = \partial_{x_k} g_i(x) = \begin{cases} -\nu\eta\,(1 - x_i)\, x_i^{\nu} + (1 - 2x_i) \left(\delta - \sum_{\substack{j=1 \\ j \neq i}}^{n} x_j^{\nu} - \eta\, x_i^{\nu} \right) & i = k \\ -\nu\,(1 - x_i)\, x_i\, x_k^{\nu - 1} & i \neq k\,. \end{cases} \tag{27}$$

Hence, for the fixed points $x = x^*$ in (24), only five type of entries are non-zero:

$$J_{11} = \cdots = J_{dd} = A := -\delta + d - 1 + \eta + e\,\psi\,, \tag{28a}$$
$$J_{d+1,d+1} = \cdots = J_{d+e,d+e} = B := -\nu\eta(1-\psi)\psi^{\nu}\,, \tag{28b}$$
$$J_{d+e+1,d+e+1} = \cdots = J_{nn} = C := \delta - d - e\,\psi\,, \tag{28c}$$
$$J_{d+1,1} = \cdots = J_{d+e,d} = D := -\nu(1-\psi)\psi\,, \tag{28d}$$
$$J_{d+e,d+1} = \cdots = J_{d+1,d+e} = E := -\nu(1-\psi)\psi^{\nu}\,, \tag{28e}$$

where $\psi = \left(\frac{\delta-d}{\eta+e-1}\right)^{1/\nu}$. Consequently, the Jabcobian is formed by four non-zero blocks,

$$J = \begin{pmatrix} J^{(a)} & 0 & 0 \\ J^{(d)} & J^{(b)} & 0 \\ 0 & 0 & J^{(c)} \end{pmatrix}. \tag{29}$$

These blocks are

$$J^{(a)} = A\,I_d\,, \tag{30a}$$
$$J^{(b)} = (B-E)\,I_e + E\,1_{e\times e}\,, \tag{30b}$$
$$J^{(c)} = C\,I_{n-d-e}\,, \tag{30c}$$
$$J^{(d)} = D\,1_{e\times d}\,, \tag{30d}$$

where I_d denotes the identity matrix of dimension d and $1_{e\times d}$ denotes the matrix of dimension $e \times d$ with all entries equal to one, etc.

The determinant of a triangular block matrix can be expressed by the product of the determinants of its block diagonal, therefore eigenvalues of the Jacobian J are given by the eigenvalues of the blocks that form the diagonal,

$$0 = \det\left(J - \lambda\,I_n\right) = \det\left(J^{(a)} - \lambda\,I_d\right)\,\det\left(J^{(b)} - \lambda\,I_e\right)\,\det\left(J^{(c)} - \lambda\,I_{n-d-e}\right). \tag{31}$$

The only non-trivial eigenvalues are those of block $J^{(b)}$, which, for $e \geq 2$, are given by

$$\begin{cases} \lambda_1^{(b)} = B + (n-1)E \\ \lambda_2^{(b)} = B - E \end{cases} \quad \text{with multiplicity} \quad \begin{cases} 1 \\ n-1\,. \end{cases}$$

Due to $B = \eta E$ and $E < 0$,

$$\lambda_1^{(b)} = (\eta + n - 1)E < 0 \qquad (\text{if } \; n + \eta > 1)\,, \tag{32}$$
$$\lambda_2^{(b)} = (\eta - 1)E > 0 \qquad (\text{if } \; \eta < 1)\,. \tag{33}$$

The second eigenvalue always has a positive sign. That is, for $e \geq 2$, all fixed points are unstable. Stable fixed points can therefore only exist if $e \leq 1$. For $e = 1$, the eigenvalue $\lambda_1^{(b)} = B$ is negative (as $\eta > 0$).

From now on, let $e \leq 1$. The eigenvalues of the two remaining blocks, $\lambda^{(a)} = A$ and $\lambda^{(c)} = C$, are negative if

$$\delta - d + 1 - \eta > e\,\psi > \delta - d\,. \tag{34}$$

For $e = 0$, the two inequalities (34) hold true if Condition (i) is met. But also for Condition (ii), which either represents the eigenvalue $\lambda^{(a)} = 0$ or the eigenvalue $\lambda^{(c)} = 0$, fixed points are stable. This is due to the premise that the limit set only contains fixed points. Namely, if the considered fixed point x^* was unstable then the solution of the dynamical system would converge to another fixed point,

$$x^+ = \big(\underbrace{1,\ldots,1}_{p},\underbrace{0,\ldots,0}_{n-p}\big)^{\mathsf{T}}, \quad \text{for which} \quad p \neq d\,. \tag{35}$$

Cases	$p \leq d-1$	$d+1 \leq p$
$d = \delta$	$\delta - p \geq 1$	$\delta - d + 1 - \eta \leq -\eta$
$d = \delta + 1 - \eta$	$\delta - p \geq \eta$	$\delta - p + 1 - \eta \leq -1$

Table 1: Relations characterizing the fixed point x^+. The relations in (34) are violated beyond equality.

If the corresponding version of Eq. (34), where d is replaced by p, was violated beyond equality (i.e., if $\delta - p \geq 0$ and $\delta - p + 1 - \eta \leq 0$) then the Jacobian would have at least one positive eigenvalue. Straightforward calculation shows that, in fact, this is the case (cf. Table 1). That is, any other fixed point x^+ would be unstable. Therefore, the considered fixed point x^* must be stable.

Note that $\lambda^{(a)} = 0$ implies $\lambda^{(c)} < 0$ and $\lambda^{(c)} = 0$ implies $\lambda^{(a)} < 0$; in both cases, $e = 0$, as the formal definition of ψ either leads to $\psi = 1/\eta > 1$ or to $\psi = 0$, respectively, contradicting (24b).

For $e = 1$, the two inequalities (34) hold true if Condition (iii) is met. In fact, the corresponding inequalities, $1 > \eta > \delta - d > 0$, lead to the inequality on the r.h.s. of (34),

$$\psi = \frac{(\delta - d)^{1/\nu}}{\eta^{1/\nu}} > (\delta - d)^{1/\nu} \geq \delta - d > 0\,. \tag{36}$$

Only if $\eta < 1/\nu$, the l.h.s. of Condition (iii) implies the inequality on the l.h.s. of (34),

$$\eta \underbrace{(\delta - d - \eta)}_{<0} \underbrace{(\nu\eta - 1)}_{<0} > 0 \tag{37}$$

$$1 - \nu(\eta - \delta + d) > \frac{\delta - d}{\eta} \tag{38}$$

$$1 > \delta - d + 1 - \eta \geq \big(1 - \nu(\eta - \delta + d)\big)^{1/\nu} > \frac{(\delta - d)^{1/\nu}}{\eta^{1/\nu}} = \psi\,. \tag{39}$$

Whenever $\eta \geq 1/\nu$, the inequality on the l.h.s. of (34) can only be true—which even applies when including equality—if $\eta \leq \delta - d$. That is,

$$\delta - d + 1 - \eta \geq \psi \quad \text{if} \quad \eta \underbrace{(\delta - d - \eta)}_{\geq 0} \underbrace{(\nu\eta - 1)}_{\geq 0} \geq 0\,. \tag{40}$$

Then, however, $\psi = \left(\frac{\delta - d}{\eta}\right)^{1/\nu} \geq 1$, which contradicts the assumption (24b) of Lemma 2.

If $\eta \geq 1/\nu$, one may represent $d \leq \delta - \eta$ through redefinition, $d \to d - 1$, as encoded by Condition (i) or (ii), and set $e = 0$. □

Corollary 3. *Let $e = 0$. Then $d = [\delta + 1 - \eta]$.*

Proof. This is an immediate consequence of the conditions (i) and (ii). □

The previous statements can be summarized as anticipated in the result section.

Theorem. *Let $d = [\delta + 1 - \eta]$ and $\psi = \min\left\{1, \max\left\{\frac{\delta - d}{\eta}, 0\right\}\right\}^{1/\nu}$. Then the solution of the ODE-system (17a) satisfying the initial conditions (17b) converges to a fixed point as $t \to \infty$. The only stable fixed point is*

$$x^* = \big(\underbrace{1, \ldots, 1}_{d}, \psi, \underbrace{0, \ldots, 0}_{n-1-d}\big)^{\mathsf{T}}\,. \tag{41}$$

Proof. Recall that the ω-limit set only consists of fixed points. The only stable fixed point for the parameters δ and η is x^*, given above. It only remains to check if the definitions of d and ψ are correct. In fact, d is defined by $[\delta + 1 - \eta]$, even if $e = 1$. Namely, if $e = 1$ then $d > \delta - \eta$, and there is only one natural number ($= d$) between $\delta - \eta$ and $\delta + 1 - \eta$. That is, the case $e = 1$ is characterized by $d = [\delta] = [\delta + 1 - \eta]$. The definition of d (i.e., $\delta - \eta < d \leq \delta + 1 - \eta$, in particular its l.h.s.) ensures that $\psi < 1$. Only if $d < \delta$, one obtains $\psi > 0$. As long as $\delta \leq d$ the theorem's premise defines the case $e = 0$ (by formally setting $\psi = 0$). □

We conclude this section by noticing another consequence of Proposition 2.

Corollary 4. *The ODE-system* (17a) *always has the following unstable fixed point,*

$$x_i^* = \left(\frac{\delta}{n-1+\eta}\right)^{1/\nu}, \quad i \leq n\,. \tag{42}$$

Proof. Let $d = 0$ and $e = n$ in Lemma 2. Then the fixed points are given by (24b). □

Acknowledgements

We would like to thank Dr. S. Butler for sending us the data that have been used in [25]. AL, JP, and SR gratefully acknowledge funding by Federal Ministry of Education and Research (BMBF) e:Bio project BovSys (FKZ031A311).

References

[1] Boer HMT, Stötzel C, Röblitz S, Deuflhard P, Veerkamp RF, Woelders H. J Theor Biol 278, 20–31 (2011).

[2] Ginther OJ, Beg MA, Bergfelt DR, Donadeu FX, Kot K. Biol Reprod 65, 639–647 (2001).

[3] Fortune JE. Biol Reprod 50, 225–232 (1994).

[4] Lacker HM. Biophys J 35, 433–454 (1981).

[5] Adams GP, Jaiswal R, Singh J, Malhi P. Theriogenology 69, 72–80 (2008).

[6] Burns DS, Jimenez-Krassel F, Ireland JLH, Knight PG, Ireland JJ. Biol Reprod 73, 54–62 (2005).

[7] Lacker HM, Beers WH, Meuli LE, Akin E. Biol Reprod 37, 570–588 (1987).

[8] Lacker HM, Percus A. J Stat Phys 63, 1133–1361 (1991).

[9] Mariana JC, Corpet F, Chevalet C. Acta Biotheoretica 42, 245–262 (1994).

[10] Soboleva TK, Peterson AJ, Pleasants AB, McNatty KP, Rhodes FM, Anim Reprod Sci 58, 45–57 (2000).

[11] Smith JF, Soboleva TK, Peterson AJ, Pleasants AB, Chagas LM, Burke CR, Proceedings of the New Zealand Society of Animal Production 65, 324–328 (2005).

[12] Selgrade JF, Harris LA, Pasteur RD. J Theor Biol 260, 572–580 (2009).

[13] Stötzel C, Plöntzke J, Heuwieser W, Röblitz S. Theriogenology 78, 1415–1428 (2012).

[14] Pring SR, Owen M, King JR, Sinclair KD, Webb R, Flint APF, Garnsworthy PC. J Theor Biol 313, 115–126 (2012).

[15] Monniaux D, Michel P, Postel M, Clement F. Biol Cell 108, 149–160 (2016).

[16] Iber D, De Geyter C. BMC Systems Biology 7, 60 (2013).

[17] Nishimoto H, Haman S, Hill GA, Miyamoto A, Tetsuka M. J Reprod Dev 55, 219–224 (2009).

[18] Macklon NS, Fauser BCJM. Archives of Medical Research 32, 595–600 (2001).

[19] Adams GP, Pierson RA. Theriogenology 43, 113–120 (1995).

[20] McGee EA, Hsueh AJW. Endocr Rev 21, 200–214 (2000).

[21] Baerwald AR, Adams GP, Pierson RA. Biol Reprod 69, 1023–1031 (2003).

[22] Panza NM, Wright AA, Selgrade JF. J Biol Dyn 10, 1 (2016).

[23] Bleach ECL, Glencross RG, Knight PG. Reproduction 127, 621–629 (2004).

[24] Wolfenson D, Inbar G, Roth Z, Kaim M, Bloch A, Braw-Tal R. Theriogenology 62, 1042–1055 (2004).

[25] Cummins SB, Lonergan P, Evans ACO, Butler ST. J Dairy Sci 95, 3698–3710 (2012).

[26] Soede NM1, Langendijk P, Kemp B. Anim Reprod Sci 124, 251–258 (2011).

[27] Greenwald GS. J Reprod Fertil 2, 351–361 (1961).

[28] Lipschütz A. British J Exp Biol 5, 283–291 (1928).

[29] Fortune JE, Rivera GM, Evans ACO, Turzillo AM. Biol Reprod 65, 648–654 (2001).

[30] Haughian JM, Ginther OJ, Diaz FJ, Wiltbank MC. Biol Reprod 88, Article 165, 1–10 (2013).

[31] Mihm M, Austin EJ. Domest Anim Endocrinol 23, 155–166 (2002).

[32] Mihm M, Evans ACO. Reprod Dom Anim 43, 48–56 (2008).

[33] Gore MA, Nayudu PL, Vlaisavljevic V. Hum Reprod 12, 2741–2747 (1997).

[34] Ginther OJ, Wiltbank MC, Fricke PM, Gibbons JR, Kot K. Biol Reprod 55, 1187–1194 (1996).

[35] Beam SW, Butler WR. J Reprod Fertil Suppl 54, 411–424 (1999).

[36] Kamel RM. J Reprod Infertil 4, 96–109 (2013).

[37] Guerra AG, Tribulo A, Yapura J, Adams GP, Singh J, Mapletoft RJ. Theriogenology 84, 467–476 (2015).

[38] Hendriksen PJM, Gadella BM, Vos PLAM, Mullaart E, Kruip TAM, Dieleman SJ. Biol Reprod 69, 2036–2044 (2003).

[39] Erickson GF, Wang C, Hsueh AJ. Nature 279, 336338 (1979).

[40] Kulick LJ, Bergfelt DR, Kot K, Ginther OJ. Biol Reprod 65, 839–846 (2001).

[41] Nagumo, M. Proceeding of the Physical-Mathematical Society, Japan, 24, 551–559 (1942).